Korean Journal of Radiology

KJR

Check for updates

Automated Breast Ultrasound: Interobserver Agreement, Diagnostic Value, and Associated Clinical Factors of Coronal-Plane Image Features

Guoxue Tang, MD[1, 2, 4, 5], Xin An, MD[1, 3], Huiling Xiang, MD[1, 2], Lixian Liu, MD[1, 2], Anhua Li, MD, PhD[1, 2], Xi Lin, MD, PhD[1, 2]

[1]State Key Laboratory of Oncology in South China and Collaborative Innovation Center for Cancer Medicine, Guangzhou, China; Departments of [2]Ultrasound and [3]Medical Oncology, Sun Yat-sen University Cancer Center, Guangzhou, China; [4]Guangdong Provincial Key Laboratory of Malignant Tumor Epigenetics and Gene Regulation, Guangzhou, China; [5]Department of Ultrasound, Sun Yat-sen Memorial Hospital, Sun Yat-sen University, Guangzhou, China

Objective: To evaluate the interobserver agreement, diagnostic value, and associated clinical factors of automated breast ultrasound (ABUS) coronal features in differentiating breast lesions.
Materials and Methods: This study enrolled 457 pathologically confirmed lesions in 387 female (age, 46.4 ± 10.3 years), including 377 masses and 80 non-mass lesions (NMLs). The unique coronal features, including retraction phenomenon, hyper- or hypoechoic rim (continuous or discontinuous), skipping sign, and white wall sign, were defined and recorded. The interobserver agreement on image type and coronal features was evaluated. Furthermore, clinical factors, including the lesion size, distance to the nipple or skin, palpability, and the histological grade were analyzed.
Results: Among the 457 lesions, 296 were malignant and 161 were benign. The overall interobserver agreement for image type and all coronal features was moderate to good. For masses, the retraction phenomenon was significantly associated with malignancies ($p < 0.001$) and more frequently presented in small and superficial invasive carcinomas with a low histological grade ($p = 0.027$, 0.002, and < 0.001, respectively). Furthermore, continuous hyper- or hypoechoic rims were predictive of benign masses ($p < 0.001$), whereas discontinuous rims were predictive of malignancies ($p < 0.001$). A hyperechoic rim was more commonly detected in masses more distant from the nipple ($p = 0.027$), and a hypoechoic rim was more frequently found in large superficial masses ($p < 0.001$ for both). For NMLs, the skipping sign was a predictor of malignancies ($p = 0.040$).
Conclusion: The coronal plane of ABUS may provide useful diagnostic value for breast lesions.
Keywords: *Breast neoplasms; Ultrasonography; Breast diseases; Diagnostic imaging*

INTRODUCTION

Breast ultrasound is a well-accepted complement to mammography in dense breasts (1). However, handheld ultrasound (HHUS) is highly operator dependent with challenges in acquiring reproducible and standardized images (2). Automated breast ultrasound (ABUS) was developed to overcome these issues (3, 4). Furthermore,

the unique coronal plane of the ABUS, which could not be generated using the conventional HHUS, may offer additional diagnostic information and potentially improve characterization of breast lesions (3, 4).

The value of coronal image features has been reported by several groups (5-12). Most studies focused on the retraction phenomenon, which had high specificity for breast malignancies (5-12). A hyperechoic rim was often

seen as a feature of benign lesions (3, 6, 9, 13, 14). To the best of our knowledge, other features, such as skipping sign, hypoechoic rim, and white wall sign, have not been reported with regard to distinguishing benign and malignant lesions. Only one study had analyzed the associated clinical factors influencing the appearance of the retraction phenomenon in invasive ductal carcinomas (IDCs) (15). The correlation between coronal features and clinical factors in the general population is still unclear.

Based on sonographic features, breast lesions are characterized into masses or non-mass lesions (NMLs). In the fifth edition of American College of Radiology Breast Imaging Reporting and Data System (BI-RADS) (16), a mass was three-dimensionally defined and occupied space, with volumetric acquisitions seen in three planes. In contrast, a NML refers to a hypoechoic area lacking a conspicuous margin or shape and can be defined as a non-space occupying lesion (17). Previous studies (18-23) have reported some features that may aid in the identification of malignant NMLs, such as palpability, architectural distortion, and calcification. However, whether the coronal features can help to evaluate NMLs has not been discussed.

Therefore, this study aimed to evaluate the interobserver agreement and diagnostic value of coronal features of ABUS in differentiating benign and malignant breast lesions based on the mass and NML types, and to investigate the associated clinical factors.

MATERIALS AND METHODS

Patients

The Institutional Review Board (approval number C2015-001-01) at our institution approved and supervised this study. Confirm that all the research meets the ethical guidelines, including adherence to the legal requirements of the study country. Since this was a retrospective study, the need to obtain an informed consent was waived. The authenticity of this paper was verified by uploading key raw data to the Research Data Deposit public platform (http://rdd.sysucc.org.cn/) with number RDDA2018000831.

We reviewed the medical records of 403 female patients who underwent conventional ultrasound-guided core needle biopsy (CNB) or surgery, and pre-operative ABUS examination from January 2016 through December 2017. Of these patients, seven women (five were confirmed as having fibrocystic changes [FCC] and two as having ductal carcinoma *in situ* [DCIS] based on pathological examination)

with negative ABUS image findings were excluded. Moreover, three patients with borderline phyllodes tumors and six patients with breast biopsy or surgery history were excluded. Finally, 387 female patients (age, 46.4 ± 10.3 years; age range, 22–74 years) with 457 breast lesions were enrolled in this study (Supplementary Fig. 1).

Chief complaints of the enrolled patients included breast pain (n = 42), nipple discharge (n = 21), palpable breast lesions (n = 198), suspicious breast lesions revealed on ultrasound (n = 73), and suspicious mammographic findings, including microcalcification and a lump (n = 53).

ABUS Image System

The Invenia™ Automated Breast Ultrasound System (GE Healthcare, Sunnyvale, CA, USA) was used. Each breast was scanned in the supine position using an automated 6–14 MHz linear broadband transducer with the following three standard planes: lateral, anteroposterior, and medial. Additional planes were obtained in cases of large breasts (cup size, D or E) to ensure adequate coverage. The depth setting of 3.5 cm, 4.5 cm, or 5 cm was selected according to the size of a patient's breast.

Definition of Image Type and Coronal Features

Each breast lesion was classified as a "mass" or "NML" based on the BI-RADS lexicon (16). Coronal features included retraction phenomenon, hyper- or hypo echoic rim (continuous or discontinuous), skipping sign, and white wall sign. Retraction phenomenon was defined as the convergence tendency of the tissue surrounding a lesion with or without cord-like hyperechogenicity intervals on the coronal plane (Figs. 1, 2) (9, 11). The skipping sign was defined as anechoic lines around the lesion (perpendicular to the probe scan direction), and the interface between the lesion and the surrounding tissues was interrupted. It used to be considered an artifact of a probe sliding over a lesion or dense breast (Figs. 2, 3) (12, 24). A video helped recognize the skipping sign associated with NMLs (Supplementary Movie 1). Continuous or discontinuous hyper- or hypoechoic rim was defined as a complete or incomplete, high or low echo boundary-like eggshell between the lesion and the surrounding tissues on the coronal plane (Figs. 4-6) (9). The continuity of a rim was evaluated using whole image slices presenting the rim. A discontinuous rim was defined as discontinuity of the rim existing on three or more consecutive planes. The default layer thickness was set at 0.5 mm, which meant that the discontinuity was required

to exceed at least 1 mm. White wall sign was defined as a white echogenic area in subsequent planes of the lesion, which was caused by posterior acoustic enhancement (Fig. 7) (12). A video helped in distinguishing the hyperechoic rim and the white wall sign (Supplementary Movie 2).

Data Collection

According to the definitions, the image type and coronal features of each lesion were interpreted by four eligible independent radiologists (with 2, 3, 5, and 15 years of experience on HHUS; and more than 1 year of experience
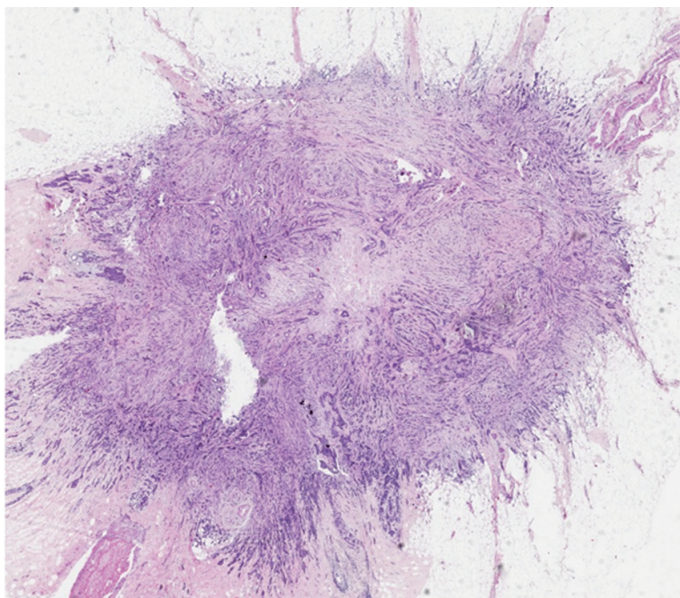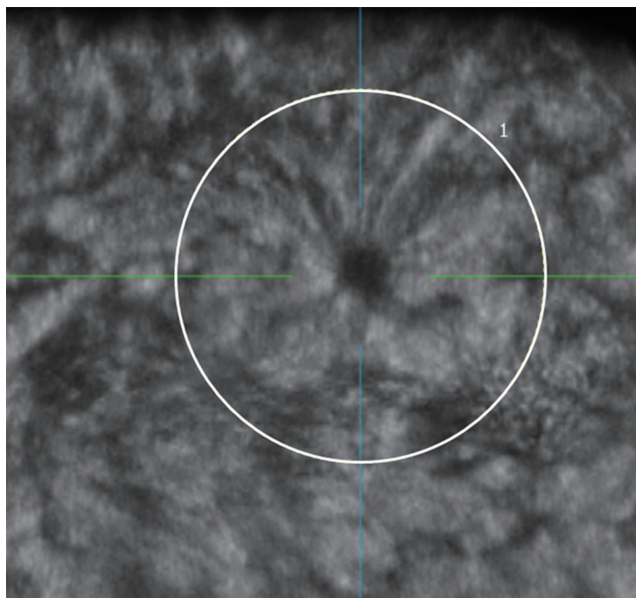
Fig. 1. Retraction phenomenon of invasive ductal carcinoma.
A. Coronal automated breast ultrasound image of 47-year-old woman with impalpable, grade II invasive ductal carcinoma (11-mm deep from skin, 75-mm far from nipple, 11-mm in size) with retraction phenomenon (circle). **B.** On corresponding pathology slide (hematoxylin-eosin stain, x 10) is central tumor with surrounding spicules pattern. Tumor is surrounded by desmoplastic changes in stroma, which reveals fibrous tissues infiltrating carcinoma cells that has alternately grown up.
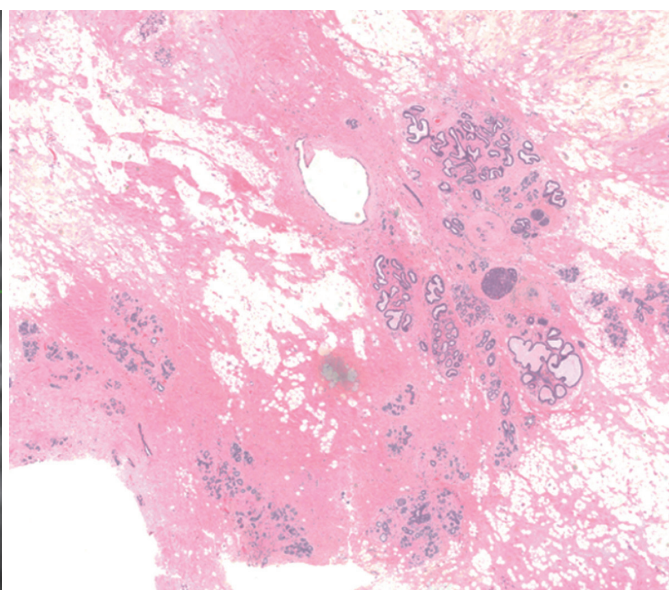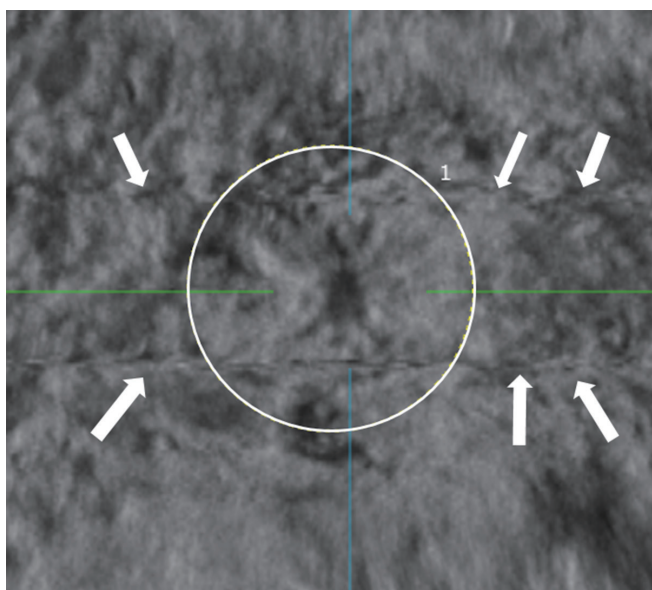
Fig. 2. Retraction phenomenon and skipping sign of sclerosing adenosis.
A. Coronal automated breast ultrasound image of 43-year-old woman with palpable, 6-mm deep from skin, 35-mm far from nipple, 15-mm in size, sclerosing adenosis with retraction phenomenon (circle) and skipping sign (arrows). **B.** On corresponding pathology slide (hematoxylin-eosin stain, x 10) are increased numbers of glands, some cystic enlarged glands at periphery and centrally located fibrosis.
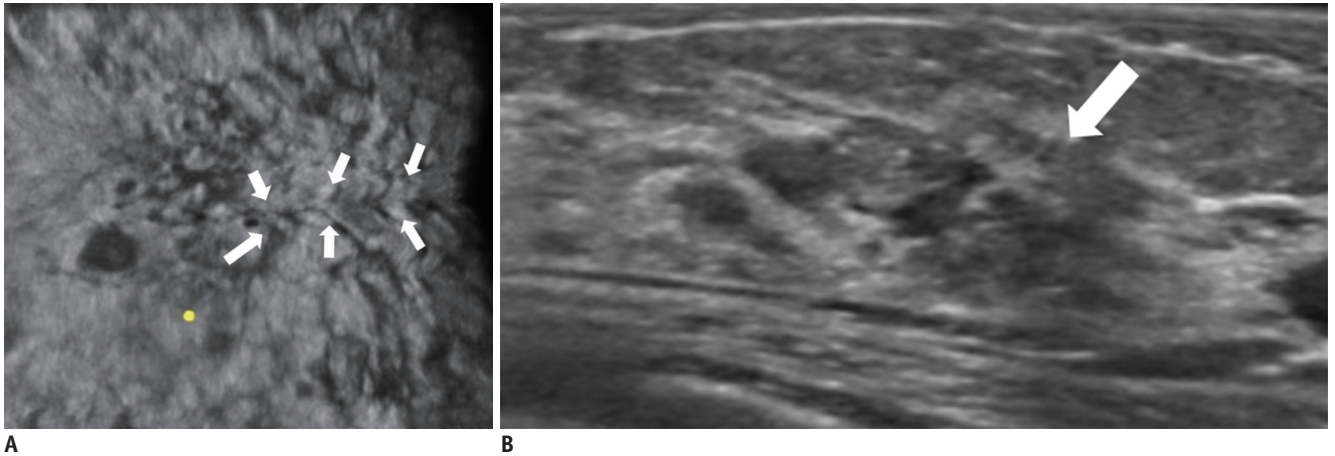
Fig. 3. Skipping sign of non-mass lesion.
Coronal **(A)** and transverse **(B)** automated breast ultrasound images of 44-year-old woman with impalpable non-mass lesion (5-mm deep from skin, 21-mm far from nipple, 39-mm in size), which displays skipping sign (arrows), and pathological result is grade I invasive ductal carcinoma associated with ductal carcinoma *in situ*. **B.** On transverse plane is diffuse hypoechoic area with microcalcifications (arrow).
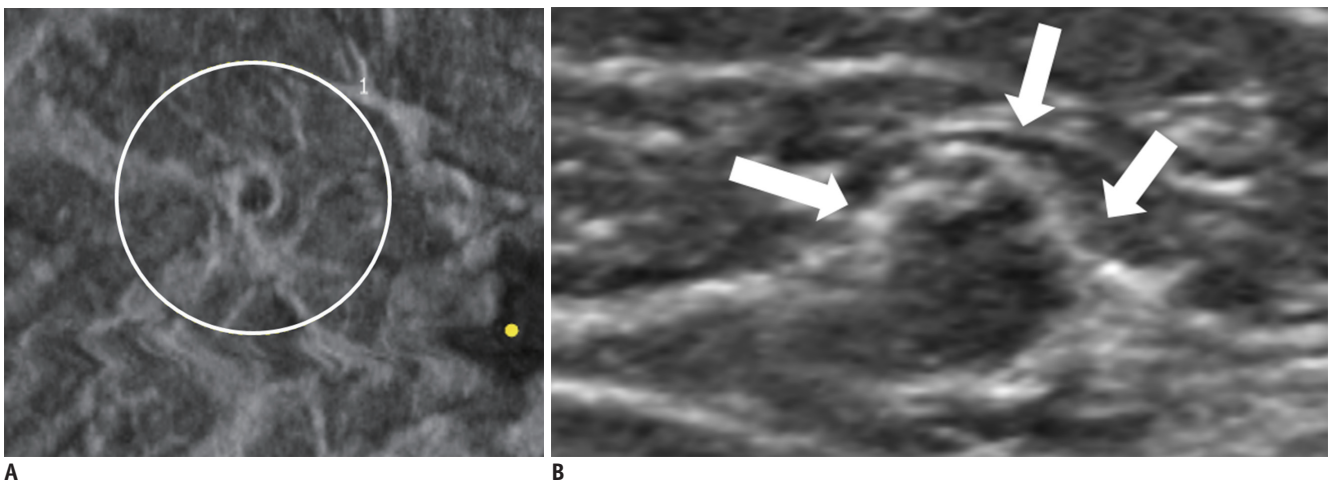
Fig. 4. Continuous hyperechoic rim of fibroadenoma.
Coronal **(A)** and transverse **(B)** automated breast ultrasound images of 44-year-old woman with impalpable fibroadenoma (36-mm deep from skin, 10-mm far from nipple, 10-mm in size) with continuous hyperechoic rim (circle). **B.** On transverse plane, above surrounding tissue is pushed by mass (arrows).

on ABUS). Cases with the same description according to three or four readers were considered as consistent. For cases with discrepancies in description among the four radiologists, agreement was reached through discussion. They were blinded to the pathological results of the target lesion and clinical information, except patient's age.

The basic clinical factors, including the longest diameter of the lesion (size), and distances from the skin and nipple were recorded in the workstation. The histological grades of IDC were assessed according to the Elston and Ellis grading system and expressed as grade I, II, or III based on post-operative samples. Histological grades I and II were regarded as low grade, whereas grade III was regarded as high grade.

Statistical Analysis

The interobserver agreement on the image type and coronal features among radiologists was assessed using kappa statistics. The kappa coefficient (κ) was interpreted as follows: poor agreement (< 20); fair agreement (0.21–0.40); moderate agreement (0.41–0.60); good agreement (0.61–0.80); and very good agreement (0.81–1.00) (25).

Chi-squared test or Fisher's exact test for categorical variables and an independent t test for continuous variables were performed to determine whether the features of the coronal planes were different between benign and malignant lesions. The sensitivity, specificity, positive predictive value, negative predictive value, and accuracy of significant coronal features were also calculated.
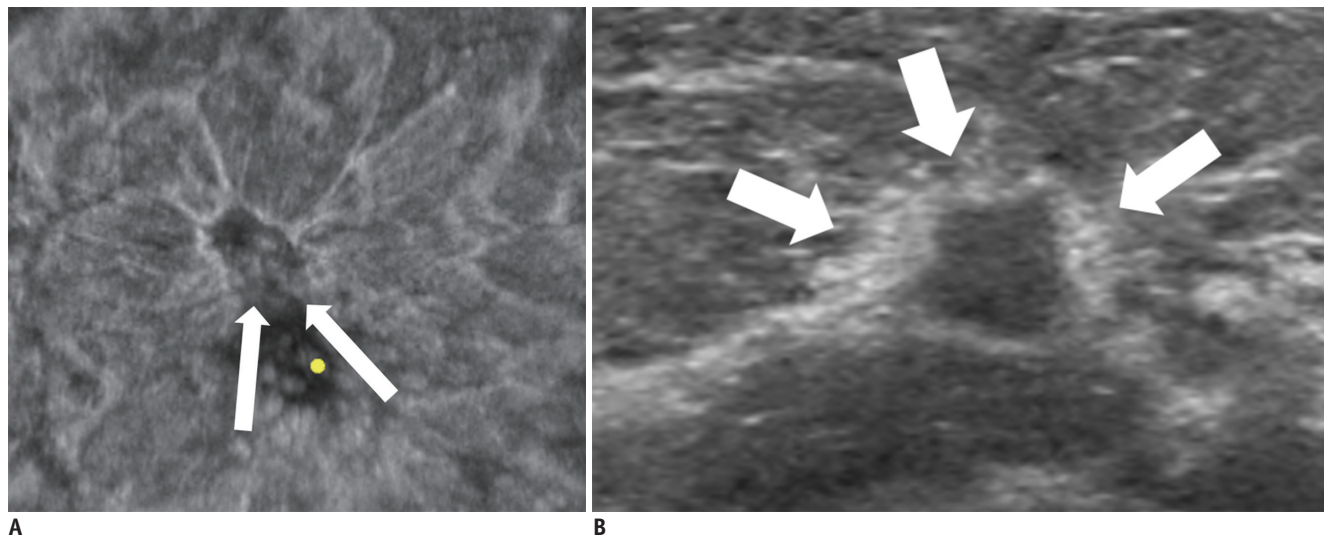
Fig. 5. Discontinuous hyperechoic rim of invasive ductal carcinoma.
Coronal **(A)** and transverse **(B)** automated breast ultrasound images of 60-year-old woman with impalpable grade II invasive ductal carcinoma (11-mm deep from skin, 24-mm far from nipple, 13-mm in size) with discontinuous hyperechoic rim (arrows; **A**). **B.** On transverse plane, discontinuous rim was caused by infiltration between tumor and surrounding tissue (arrows).
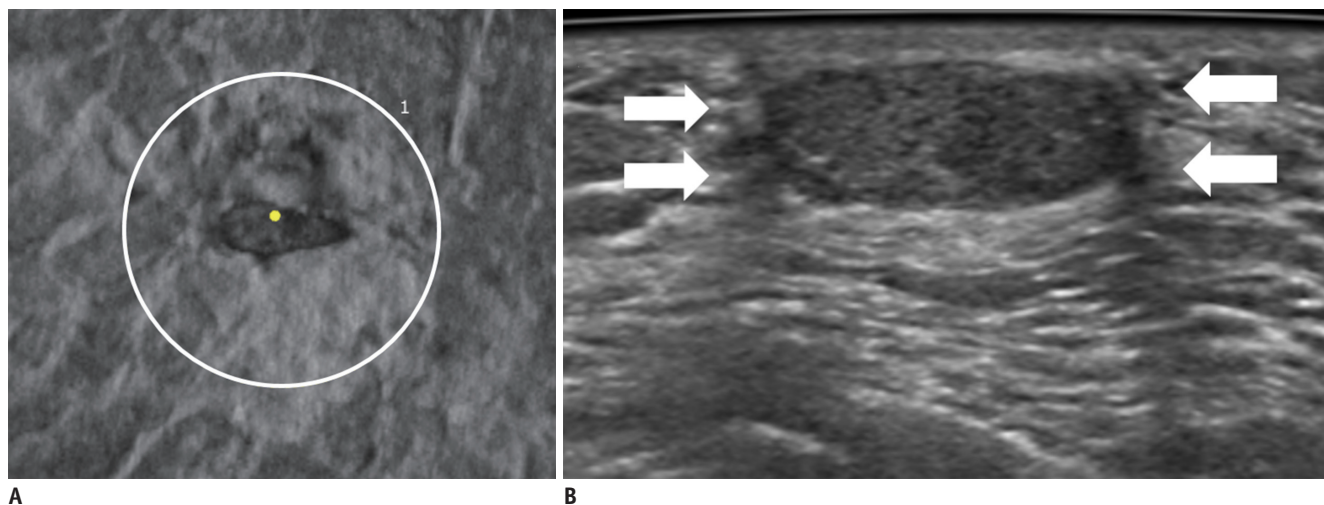
Fig. 6. Continuous hypoechoic rim of fibroadenoma.
Coronal **(A)** and transverse **(B)** automated breast ultrasound images of 34-year-old woman with palpable fibroadenoma (4-mm deep from skin, under nipple, 23-mm in size) with continuous hypoechoic rim (circle). **B.** On transverse plane, hypoechoic rim was caused by lateral acoustic shadow (arrows).

Statistically significant clinical factors (including palpation, lesion size, distance to skin or nipple, and histological grade) for coronal features based on the univariate analysis were selected for multivariate analysis (logistic regression) and the association results were expressed as odds ratios and 95% confidence intervals.

All statistical analyses were performed using SPSS (version 19.0, IBM Corp., Armonk, NY, USA) and Stata statistical package (release 15.0, StataCorp LLC, College Station, TX, USA). A p value less than 0.05 was considered as statistically significant.

RESULTS

Clinical Characteristics and Pathological Results of Enrolled Lesions

The correlation of pathological results and ultrasound image types are described in Table 1. Of the 457 lesions, 161 (35.2%) were benign (including high-risk lesions: atypical ductal hyperplasia and lobular carcinoma *in situ*) and 296 (64.8%) were malignant. Ninety lesions were confirmed by HHUS-guided CNB, and 367 lesions were confirmed during surgery. All malignancies, intraductal

A

B
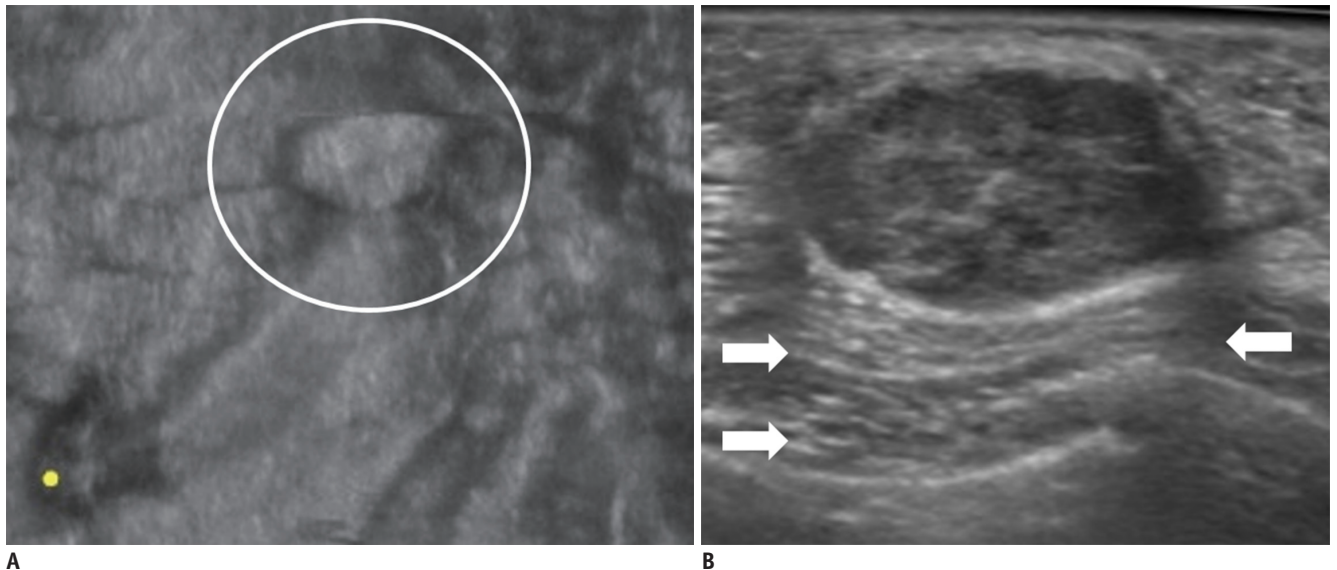
Fig. 7. White wall sign of fibroadenoma.
Coronal **(A)** and transverse **(B)** automated breast ultrasound images of 35-year-old woman with palpable fibroadenoma (5-mm deep from skin, 58-mm far from nipple, 23-mm in size) with white wall sign (circle). **B.** On transverse plane, white wall sign was associated with posterior enhancement (arrows).

Table 1. Summary of Pathological Outcomes, and Image Types for 457 Breast Lesions

Pathology	Image Types		Total
	Masses	NMLs	
Benign			
FCC	47	27	74
Mastitis	9	0	9
Fibroadenoma	56	4	60
ADH	1	1	2
IDP	6	2	8
Benign phyllodes tumor	5	0	5
LCIS	0	3	3
Malignant			
DCIS	7	15	22
IDC	177	12	189
DCIS + IDC	53	13	66
ILC	9	2	11
Malignant phyllodes tumor	0	1	1
Mucinous CA	3	0	3
Medullay CA	1	0	1
Papillary CA	2	0	2
Metaplastic CA	1	0	1
Total	377	80	457

ADH = atypical ductal hyperplasia, CA = carcinoma, DCIS = ductal carcinoma *in situ*, FCC = fibrocystic changes, including fibrosis, sclerosing adenosis, and apocrine metaplasia, IDC = invasive ductal carcinoma, IDP = intraductal papilloma, ILC = invasive lobular carcinoma, LCIS = lobular carcinoma *in situ*, NMLs = non-mass lesions

papilloma, and high-risk lesions were confirmed by surgery.

In the mass group, 206 lesions (55%) were palpable. Median lesion size and distance to the skin and nipple were 18.5 mm (range, 5–63 mm), 7.3 mm (range, 2–20 mm), and 40.2 mm (0–89 mm), respectively. IDCs included 108 low-grade IDCs, 98 high-grade IDCs and 21 unknown ones. In the NML group, 27 lesions (34%) were palpable. Median lesion size, distance to the skin and nipple were 26.0 mm (range, 6–70 mm), 7.0 mm (range, 2–15 mm), and 34.5 mm (0–70 mm), respectively. IDCs included 17 low-grade IDCs, eight high-grade IDCs, and three unknown ones. The unknown lesions included IDCs that only underwent biopsy (n = 19) and neoadjuvant chemotherapy before the surgery (n = 5).

Interobserver Agreement

Table 2 listed the results of interobserver agreement on image type and coronal features. The overall interobserver agreements among radiologists for image type, retraction phenomenon, skipping sign, hyperechoic rim, hypoechoic rim, and white wall sign were 0.678, 0.681, 0.588, 0.486, 0.621, and 0.567, respectively.

Diagnostic Value of Coronal Features

Table 3 showed the correlation of coronal features with pathological results and Table 4 described the diagnostic accuracy of coronal features.

Among masses, the malignant masses were associated with retraction phenomenon and discontinuous hyper- and hypoechoic rim ($p < 0.001$ for each). The correct

Table 2. Interobserver Agreement on Image Type and Coronal Features of Enrolled Lesions

Features	Subgroup	κ Value
Image type		0.678
Retraction phenomenon		0.681
Skipping sign		0.588
Hyperechoic rim	No	0.537
	Continuous	0.447
	Discontinuous	0.437
	Overall	0.486
Hypoechoic rim	No	0.708
	Continuous	0.631
	Discontinuous	0.297
	Overall	0.621
White wall sign		0.567

κ = kappa coefficient

categorization of malignant masses of retraction phenomenon, discontinuous hyper-, and hypoechoic rims had sensitivity and specificity values of: 42.3% and 91.1%; 28.5% and 95.2%; and 8.3% and 96.8%, respectively. Benign masses were associated with continuous hyper- and hypoechoic rims ($p < 0.001$ for both). Both the continuous hyper- and hypoechoic rims had high specificity (90.1% and 92.1%, respectively) and relatively low sensitivity (26.6% and 33.1%, respectively) in the correct categorization of benign masses.

Among NMLs, the malignant NMLs were associated with a skipping sign ($p = 0.040$), which had high specificity (89.2%) and a relatively low sensitivity (32.6%). Neither a hyper/hypoechoic rim nor a white wall sign was detected in any NML.

Associated Clinical Factors

Table 5, Supplementary Tables 1 and 2 describe the

Table 3. Summary of Correlation between Coronal Features and Pathological Results

Variables	Mass Group (n = 377)				NML Group (n = 80)			
	Benignity (%)	Malignancy (%)	P	Total	Benignity (%)	Malignancy (%)	P	Total
Retraction phenomenon			< 0.001				0.074	
No	113 (44)	146 (56)		259	34 (52)	32 (48)		66
Yes	11 (9)	107 (91)		118	3 (21)	11 (79)		14
Skipping Sign			0.105				0.040	
No	101 (35)	187 (65)		288	33 (53)	29 (47)		62
Yes	23 (26)	66 (74)		89	4 (22)	14 (78)		18
Hyperechoic halo			< 0.001				-	
No	85 (35)	156 (65)		241	37 (100)	43 (100)		80
Continuous	33 (57)	25 (43)		58	0	0		0
Discontinuous	6 (8)	72 (92)		78	0	0		0
Hypoechoic halo			< 0.001				-	
No	79 (27)	212 (73)		291	37 (100)	43 (100)		80
Continuous	41 (67)	20 (33)		61	0	0		0
Discontinuous	4 (16)	21 (84)		25	0	0		0
White wall sign			0.161				-	
No	90 (31)	200 (69)		290	37 (100)	43 (100)		80
Yes	34 (39)	53 (61)		87	0	0		0

Table 4 Summary of Diagnostic Value of Coronal Features in Distinguishing of Benign and Malignant Breast Lesions

Coronal Features	Sen (%)	Spe (%)	PPV (%)	NPV (%)	Accuracy (%)
Masses (n = 377)					
Retraction phenomenon for malignancy	42.3	91.1	90.7	43.6	58.4
Discontinuous hyperechoic rim for malignancy	28.5	95.2	92.3	39.5	50.4
Discontinuous hypoechoic rim for malignancy	8.3	96.8	84.0	34.1	37.4
Continuous hyperechoic rim for benignity	26.6	90.1	56.9	71.5	69.2
Continuous hypoechoic rim for benignity	33.1	92.1	67.2	73.7	72.7
NMLs (n = 80)					
Skipping sign for malignancy	32.6	89.2	77.8	53.2	58.8

NPV = negative predictive value, PPV = positive predictive value, Sen = sensitivity, Spe = specificity

Table 5. Summary of Binary Logistic Regression Results of Clinical Factors for Appearance of Coronal Features

Coronal Features	Clinical Factors	P	Odds Ratio (95% CI)
Masses			
Retraction phenomenon	Pathological results	< 0.001	7.53 (3.86–14.68)
Skipping sign	Palpable	0.001	2.91 (1.52–5.57)
	Size	< 0.001	1.06 (1.03–1.09)
	Distance to skin	0.010	0.89 (0.81–0.97)
Hyperechoic rim	Distance to nipple	0.027	1.01 (1.00–1.02)
Hypoechoic rim	Palpable	0.670	1.01 (0.98–1.04)
	Size	< 0.001	3.64 (1.87–7.11)
	Distance to skin	< 0.001	0.84 (0.76–1.04)
	Pathological results	< 0.001	0.23 (0.13–0.41)
White wall sign	Palpable	0.054	1.81 (0.99–3.31)
	Size	< 0.001	1.06 (1.03–1.09)
	Distance to skin	0.096	0.93 (0.86–1.01)
NMLs			
Skipping sign	Pathological results	0.026	3.98 (1.18–13.46)

Only variables with significant differences in univariate analysis are shown. Supplementary Tables 1 and 2 shows complete results of this analysis. CI = confidence interval

correlation between the appearance of coronal features and clinical factors. In the masses group, multivariate analysis revealed that the pathological result was the sole factor affecting the appearance of the retraction phenomenon ($p < 0.001$). Palpation, mass size, and the distance to the skin were independent factors affecting the appearance of skipping sign (p values: < 0.001, < 0.001, and 0.010, respectively). The distance to the nipple was the only independent factor affecting the appearance of hyperechoic rim ($p = 0.027$). Mass size, distance to the skin, and pathological results were independent factors affecting the appearance of hyperechoic rim ($p < 0.001$ for each). Only mass size was the independent factor affecting the appearance of white wall sign ($p < 0.001$).

Regarding the appearance of retraction phenomenon in the NML group, there were no statistical findings in any clinical factor. The pathological result was the sole independent factor for the appearance of skipping sign ($p = 0.026$).

In malignant masses, retraction phenomenon was more commonly detected in masses of small size, short distance to the skin and low histological grade (p values: 0.027, 0.002, and < 0.001, respectively). In malignant NMLs, there was no statistical difference between any clinical factors regarding the appearance of the skipping sign.

DISCUSSION

Our study included ABUS images of 457 lesions and found

that the retraction phenomenon, hyper- or hypoechoic rim, skipping sign, and white wall sign of the coronal plane were useful in distinguishing benign from malignant breast lesions. In this study, the incidence of NMLs was much lower than that of masses in consecutive women (18, 19, 21, 23), with a rate of approximately 1:5 (80:377). Additionally, the coronal ABUS image features were correlated with the clinical factors according to lesion type. These results indicated that retraction phenomenon was a predictor for malignant masses, while the skipping sign was associated with malignant NMLs. Neither the echogenic rim nor the white wall sign was detected in any NML. The pathological composition of masses and NMLs were also different. In our series, malignancies were more frequent in patients with masses (67.1%) than in those with NMLs (53.8%). Fibroadenoma (45.2%) and IDC (89.3%) were the most common pathological results of benign and malignant masses. Nevertheless, FCC (73.0%) and DCIS (65.1%) were the most common breast diseases of benign and malignant NMLs.

In this study, the overall interobserver agreement for image type and all coronal features was moderate to good (κ, 0.44–0.71), and the interobserver agreement for retraction phenomenon ($\kappa = 0.68$) was slightly higher than that in a previous study ($\kappa = 0.54$) (26). This suggested that the definition and classification of image and coronal features were easy to understand and user-friendly, even for less-experienced doctors. A relatively low agreement was achieved for overall hyperechoic rims ($\kappa = 0.49$), and a fair agreement was obtained for discontinuous hypoechoic

rims (κ = 0.30). It was a challenge to accurately interpret the continuity of the rims, which required careful layer-by-layer observation and plenty of exercise. Another reason for the low agreement was that only 25 lesions presented discontinuous hypoechoic rims.

For masses, retraction phenomenon caused by tumor infiltration and surrounding tissue response changes (10) had high specificity (91.1%) and was a strong predictor of malignancy. A slightly lower sensitivity (42.3%) of retraction phenomenon was found in our study, compared to the previously reported values (55–91%) (6, 8-11, 13-15, 27) . A possible reason was the lack of a standardized definition of the retraction phenomenon, which was also interpreted in various studies as a convergence sign, stellate lesion, pattern or margin, or architectural distortion (6, 7, 28). Jiang et al. (15) and our data showed that the smaller and more superficial invasive carcinomas with lower histological grades tended to present with retraction phenomenon. Therefore, another possible reason contributing to the low sensitivity was the relatively large mean diameter (19.5 mm) of malignant masses in our group. It is worth mentioning that this feature can also be detected in sclerosing adenosis (Fig. 2) (11, 12).

A skipping sign, also called a partial deletion artifact or skip artifact (3, 10, 12), is caused by the disruption of the scanning process. It indicates the presence of a palpable lesion, nipple, or dense breast tissue, and could sometimes affect image interpretation. Our study showed that the skipping sign was more commonly seen in a palpable, superficial, or lager size mass. It had no value in distinguishing malignancies in the mass group.

A hyperechoic rim, also known as converging pattern (13, 27), is caused by the compressed fibrous surrounding tissue or the infiltration between the tumor and the surrounding tissue (9). Hypoechoic rim, first assessed in this study, is a lateral acoustic shadow caused by the smooth margin of the mass. Both continuous rims appear as characteristics identifying a benign mass, such as fibroadenomas, presenting with a circumscribed regular margin (6, 13). In contrast, a discontinuous rim is suggestive of malignancy. In this study, 90.4% of masses displaying a discontinuous hyper- or hypoechoic rim or both, were malignant, including 80 IDCs, two invasive lobular carcinomas (ILCs), and one each of medullary carcinoma, papillary carcinoma, and mucinous carcinoma. On further analysis, it was easier to detect the hyperechoic rim with an increased distance from the nipple, perhaps due to a more obvious contrast with

the hypoechoic fat tissue as the breast tissue got thinner. Besides, the hypoechoic rim was more frequently detected in large superficial masses, which was potentially related to better display of the lateral acoustic shadow in the area near the skin and in larger masses.

Posterior echo enhancement was seen as a 'white wall sign' in the coronal plane (12, 29), which is easier to observe in large-size masses, mostly associated with benign cysts, and showed no value in diagnostic differentiation for breast masses. Indeed, various malignant tumors can also possess this sign, as long as the tumor is homogeneous and well acoustic transmitted, or with cystic components. The posterior feature was not an effective predictor of differentiation (11).

For NMLs, there was no statistical significance of retraction phenomenon in our study and this had several possible reasons. First, the mean size of malignant NMLs was 32.0 mm, which was much larger than that of masses of 19.5 mm and may have reduced the chance of presenting the retraction phenomenon. Second, it was difficult to define the true margin between NML and the surrounding tissues due to the diffuse nature, thereby affecting the interpretation of the retraction phenomenon. Finally, previous studies had reported that retraction phenomenon was a strong predictor only for invasive cancers (8, 10). In this study, a higher proportion of noninvasive cancers were included in NMLs than in masses.

The skipping sign was a predictor for malignant NMLs (Fig. 3) with a high specificity (89.2%) and a relatively low sensitivity (32.6%). Overall, 18 NMLs showed skipping signs as follows: ten IDCs (four cases with DCIS), three DCIS, three FCCs, one ILC, and one fibroadenoma. There was no statistical difference between the clinical factors and the presence of skipping sign in malignant NMLs.

This study had limitations. Firstly, this was a retrospective report based on samples from a single cancer center. Furthermore, the number of malignant cases enrolled was relatively high and may have introduced sample bias and participation bias (30). Secondly, the number of NML samples was relatively small. Further study with more NMLs is needed to test the diagnostic value of coronal features of ABUS. Thirdly, an image-based selection bias (30) could not be completely avoided because the enrolled cases must have undergone ABUS exam, biopsy, or surgery. Our results need to be validated in prospective multicenter studies with a large screening population.

In conclusion, the coronal plane of ABUS may provide

additional diagnostic value for breast lesions. In the mass group, the retraction phenomenon predicted malignancy; continuous hyper- or hypoechoic rims were benign features, whereas discontinuous rims were predictive of malignancies. In the NML group, the skipping sign may help detect malignant lesions.

Supplementary Materials

The Data Supplement is available with this article at https://doi.org/10.3348/kjr.2019.0525.

Supplementary Movie Legends

Movie 1. Skipping sign of non-mass lesion.
Automated breast ultrasound volume (left anteroposterior) of a 44-year-old woman with an impalpable non-mass lesion (12 o'clock, 5-mm deep from skin, 21-mm far from nipple, 39-mm in size) presenting skipping sign. The pathological result is grade I invasive ductal carcinoma associated with ductal carcinoma *in situ*.

Movie 2. Differentiation of hyperechoic rim and white wall sign.
Automated breast ultrasound volume (left lateral) of a 35-year-old woman with a palpable fibroadenoma (1 o'clock, 5-mm deep from skin, 58-mm far from nipple, 23-mm in size). It may look like a hyperechoic rim at the first sight (about 1.6 s). However, from a dynamic observation, it is a part of posterior enhancement in the subsequent planes, which finally continues into the white wall sign. Continuous hypoechoic rim and skipping sign are also presented.

Conflicts of Interest
The authors have no potential conflicts of interest to disclose.

ORCID iDs
Xi Lin
　https://orcid.org/0000-0003-2984-1703
Guoxue Tang
　https://orcid.org/0000-0002-1945-0445
Xin An
　https://orcid.org/0000-0003-0683-5511
Huiling Xiang
　https://orcid.org/0000-0001-5734-4080
Lixian Liu
　https://orcid.org/0000-0002-2877-5583
Anhua Li
　https://orcid.org/0000-0002-4157-7805

REFERENCES

1. Shen S, Zhou Y, Xu Y, Zhang B, Duan X, Huang R, et al. A multi-centre randomised trial comparing ultrasound vs mammography for screening breast cancer in high-risk Chinese women. *Br J Cancer* 2015;112:998-1004
2. Sprague BL, Stout NK, Schechter C, van Ravesteyn NT, Cevik M, Alagoz O, et al. Benefits, harms, and cost-effectiveness of supplemental ultrasonography screening for women with dense breasts. *Ann Intern Med* 2015;162:157-166
3. Rella R, Belli P, Giuliani M, Bufi E, Carlino G, Rinaldi P, et al. Automated breast ultrasonography (ABUS) in the screening and diagnostic setting: indications and practical use. *Acad Radiol* 2018;25:1457-1470
4. Kim SH, Kim HH, Moon WK. Automated breast ultrasound screening for dense breasts. *Korean J Radiol* 2020;21:15-24
5. Kotsianos-Hermle D, Hiltawsky KM, Wirth S, Fischer T, Friese K, Reiser M. Analysis of 107 breast lesions with automated 3D ultrasound and comparison with mammography and manual ultrasound. *Eur J Radiol* 2009;71:109-115
6. Wang ZL, Xu JH, Li JL, Huang Y, Tang J. Comparison of automated breast volume scanning to hand-held ultrasound and mammography. *Radiol Med* 2012;117:1287-1293
7. Wang HY, Jiang YX, Zhu QL, Zhang J, Dai Q, Liu H, et al. Differentiation of benign and malignant breast lesions: a comparison between automatically generated breast volume scans and handheld ultrasound examinations. *Eur J Radiol* 2012;81:3190-3200
8. Lin X, Wang J, Han F, Fu J, Li A. Analysis of eighty-one cases with breast lesions using automated breast volume scanner and comparison with handheld ultrasound. *Eur J Radiol* 2012;81:873-878
9. Chen L, Chen Y, Diao XH, Fang L, Pang Y, Cheng AQ, et al. Comparative study of automated breast 3-D ultrasound and handheld B-mode ultrasound for differentiation of benign and malignant breast masses. *Ultrasound Med Biol* 2013;39:1735-1742
10. Xiao Y, Zhou Q, Chen Z. Automated breast volume scanning versus conventional ultrasound in breast cancer screening. *Acad Radiol* 2015;22:387-399
11. Zheng FY, Yan LX, Huang BJ, Xia HS, Wang X, Lu Q, et al. Comparison of retraction phenomenon and BI-RADS-US descriptors in differentiating benign and malignant breast masses using an automated breast volume scanner. *Eur J Radiol* 2015;84:2123-2129
12. Vourtsis A, Kachulis A. The performance of 3D ABUS versus HHUS in the visualisation and BI-RADS characterisation of breast lesions in a large cohort of 1,886 women. *Eur Radiol* 2018;28:592-601
13. Rotten D, Levaillant JM, Zerat L. Analysis of normal breast

tissue and of solid breast masses using three-dimensional ultrasound mammography. *Ultrasound Obstet Gynecol* 1999;14:114-124

14. Watermann DO, Földi M, Hanjalic-Beck A, Hasenburg A, Lüghausen A, Prömpeler H, et al. Three-dimensional ultrasound for the assessment of breast lesions. *Ultrasound Obstet Gynecol* 2005;25:592-598

15. Jiang J, Chen YQ, Xu YZ, Chen ML, Zhu YK, Guan WB, et al. Correlation between three-dimensional ultrasound features and pathological prognostic factors in breast cancer. *Eur Radiol* 2014;24:1186-1196

16. American College of Radiology. *BI-RADS: ultrasound. Breast imaging reporting and data system atlas*, 5th ed. Reston: American College of Radiology, 2013

17. Uematsu T. Non-mass-like lesions on breast ultrasonography: a systematic review. *Breast Cancer* 2012;19:295-301

18. Ko KH, Jung HK, Kim SJ, Kim H, Yoon JH. Potential role of shear-wave ultrasound elastography for the differential diagnosis of breast non-mass lesions: preliminary report. *Eur Radiol* 2014;24:305-311

19. Wang ZL, Li N, Li M, Wan WB. Non-mass-like lesions on breast ultrasound: classification and correlation with histology. *Radiol Med* 2015;120:905-910

20. Ko KH, Hsu HH, Yu JC, Peng YJ, Tung HJ, Chu CM, et al. Non-mass-like breast lesions at ultrasonography: feature analysis and BI-RADS assessment. *Eur J Radiol* 2015;84:77-85

21. Choi JS, Han BK, Ko EY, Ko ES, Shin JH, Kim GR. Additional diagnostic value of shear-wave elastography and color Doppler US for evaluation of breast non-mass lesions detected at B-mode US. *Eur Radiol* 2016;26:3542-3549

22. Park JW, Ko KH, Kim EK, Kuzmiak CM, Jung HK. Non-mass breast lesions on ultrasound: final outcomes and predictors of malignancy. *Acta Radiol* 2017;58:1054-1060

23. Park SY, Choi JS, Han BK, Ko EY, Ko ES. Shear wave elastography in the diagnosis of breast non-mass lesions: factors associated with false negative and false positive results. *Eur Radiol* 2017;27:3788-3798

24. Kim SH. Image quality and artifacts in automated breast ultrasonography. *Ultrasonography* 2019;38:83-91

25. Landis JR, Koch GG. The measurement of observer agreement for categorical data. *Biometrics* 1977;33:159-174

26. Zhang J, Lai XJ, Zhu QL, Wang HY, Jiang YX, Liu H, et al. Interobserver agreement for sonograms of breast lesions obtained by an automated breast volume scanner. *Eur J Radiol* 2012;81:2179-2183

27. Kalmantis K, Dimitrakakis C, Koumpis Ch, Tsigginou A, Papantoniou N, Mesogitis S, et al. The contribution of three-dimensional power Doppler imaging in the preoperative assessment of breast tumors: a preliminary report. *Obstet Gynecol Int* 2009;2009:530579

28. van Zelst JCM, Balkenhol M, Tan T, Rutten M, Imhof-Tas M, Bult P, et al. Sonographic phenotypes of molecular subtypes of invasive ductal cancer in automated 3-D breast ultrasound. *Ultrasound Med Biol* 2017;43:1820-1828

29. Brem RF, Tabár L, Duffy SW, Inciardi MF, Guingrich JA, Hashimoto BE, et al. Assessing improvement in detection of breast cancer with three-dimensional automated breast US in women with dense breast tissue: the somoInsight study. *Radiology* 2015;274:663-673

30. Sica GT. Bias in research studies. *Radiology* 2006;238:780-789